Molecular Biology of the Cell
Vol. 13, 3508–3520, October 2002

High-Resolution Dissection of Phagosome Maturation Reveals Distinct Membrane Trafficking Phases

Daniel Gotthardt,* Hans Jörg Warnatz,* Oliver Henschel,† Franz Brückert,‡ Michael Schleicher,§ and Thierry Soldati*‖¶

Departments of *Molecular Cell Research and †Cell Physiology, Max-Planck-Institute for Medical Research, D-69120 Heidelberg, Germany; ‡Laboratoire de Biochimie et Biophysique des Systèmes Intégrés, UMR5092-CNRS, CEA, 38054 Grenoble, France; §Institute of Cell Biology, Ludwig-Maximilians University, D-80336 Munich, Germany; and ‖Department of Biological Sciences, Alexander Fleming Building, Imperial College of Science Technology and Medicine, London SW7 2AZ, UK

Submitted April 18, 2002; Revised July 2, 2002; Accepted July 18, 2002
Monitoring Editor: Peter N. Devreotes

Molecular mechanisms of endocytosis in the genetically and biochemically tractable professional phagocyte *Dictyostelium discoideum* reveal a striking degree of similarity to higher eukaryotic cells. Pulse-chase feeding with latex beads allowed purification of phagosomes at different stages of maturation. Gentle ATP stripping of an actin meshwork entrapping contaminating organelles resulted in a 10-fold increase in yield and purity, as confirmed by electron microscopy. Temporal profiling of signaling, cytoskeletal, and trafficking proteins resulted in a complex molecular fingerprint of phagosome biogenesis and maturation. First, nascent phagosomes were associated with coronin and rapidly received a lysosomal glycoprotein, LmpB. Second, at least two phases of delivery of lysosomal hydrolases (cathepsin D [CatD] and cysteine protease [CPp34]) were accompanied by removal of plasma membrane components (PM4C4 and biotinylated surface proteins). Third, a phase of late maturation, preparing for final exocytosis of undigested material, included quantitative recycling of hydrolases and association with vacuolin. Also, lysosomal glycoproteins of the Lmp family showed distinct trafficking kinetics. The delivery and recycling of CatD was directly visualized by confocal microscopy. This heavy membrane traffic of cargos was precisely accompanied by regulatory proteins such as the Rab7 GTPases and the endosomal SNAREs Vti1 and VAMP7. This initial molecular description of phagocytosis demonstrates the feasibility of a comprehensive analysis of phagosomal lipids and proteins in genetically modified strains.

INTRODUCTION

Phagocytosis is prominent in leukocytes, macrophages, and dendritic cells and is involved in host defense, immunological reactions, macromolecular transport, the regulation of metabolic pathways, and signal transduction. In addition, phagocytic clearance of cell corpses generated by programmed cell death has an essential role in tissue homeostasis. A basic description of phagocytosis, an uptake mechanism based on a complex rearrangement of the actin cytoskeleton delivering large particles into intracellular vacuoles, has been available since the seminal studies of Metchnikoff (1905), but the molecular mechanisms are only beginning to be elucidated. It is usually initiated by the interaction of particle-bound ligands with receptors on the surface of professional phagocytes, such as macrophages and neutrophils. Among the surface proteins dedicated to phagocytosis, Fc receptors (FcRs) and receptors for complement (CRs) mediate the clearance of pathogens opsonized by specific antibody or complement, respectively. FcR- and CR-mediated phagocytosis appear morphologically different (Chimini and Chavrier, 2000), but both signaling pathways lead to activation of small Rho GTPases (Caron and

Article published online ahead of print. Mol. Biol. Cell 10.1091/mbc.E02–04–0206. Article and publication date are at www.molbiolcell.org/cgi/doi/10.1091/mbc.E02–04–0206.

¶Corresponding author. E-mail address: t.soldati@ic.ac.uk.

Abbreviations used: CatD, cathepsin D; CPp34, cysteine protease of 34 kDa; CR, receptor for complement; ER, endoplasmic reticulum; ESI, electrospray ionization; FcR, Fc receptor; HRP, horseradish peroxidase; IFA, immunofluorescence assay; LB, latex beads; mAb, monoclonal antibody; MS, mass spectrometry; pAb, polyclonal antibody; PC, phosphatidylcholine; PE, phosphatidylethanolamine; V-ATPase, vacuolar ATPase.

Hall, 1998). A functional actin cytoskeleton is necessary for phagocytosis (Allison *et al.*, 1971), and during FcR-mediated uptake, ruffles contain actin and actin-associated proteins (Allen and Aderem, 1995; Castellano *et al.*, 2001). Recent studies indicate that a myosin contractile activity for purse closure accompanies phagocytosis (Swanson *et al.*, 1999). In addition, membrane is added focally to the phagocytic cup to meet the significant requirements of new membrane to surround the particle (Booth *et al.*, 2001). The reservoir of membrane appears to be a Rab11- (Cox *et al.*, 2000) and COPI-dependent (Hackam *et al.*, 2001) endosomal compartment positive for VAMP3 (Bajno *et al.*, 2000).

The molecular machinery governing membrane interactions in the phagocytic apparatus has been studied extensively. Soon after formation, phagosomes modify their composition by recycling plasma membrane molecules (Muller *et al.*, 1983) and by acquiring markers of the early endocytic pathway (Pitt *et al.*, 1992; Desjardins *et al.*, 1994a). Maturing phagosomes sequentially acquire markers of late endosomes and lysosomes (Pitt *et al.*, 1992; Desjardins *et al.*, 1994b; Jahraus *et al.*, 1994; Oh *et al.*, 1996; Claus *et al.*, 1998; Ramachandra *et al.*, 1999). Sequential acquisition of hydrolases suggests that they are acquired through successive fusion with distinct endosomes (Claus *et al.*, 1998). According to the kiss-and-run hypothesis (Desjardins, 1995), phagosomes and endosomes move along cytoskeletal elements and interact at focal points at which fusion events occur. Cell-free assays confirmed the ability of phagosomes to move bidirectionally along microtubules (Blocker *et al.*, 1997). Their capacity to nucleate and interact with actin filaments plays a crucial role in their biogenesis (Defacque *et al.*, 2000; Jahraus *et al.*, 2001). Changes in phospholipid composition are also observed during maturation (Desjardins *et al.*, 1994a).

Dictyostelium discoideum, a cellular amoeba that originally lived on the forest floor feeding on bacteria and yeast, has unique advantages as a model system to investigate endocytic processes. Laboratory strains have phagocytosis rates 2-fold to 10-fold higher than those observed in macrophages or neutrophils (Thilo, 1985), and the molecular mechanisms of endocytic membrane trafficking have been well investigated in recent years (for review, see Maniak, 1999; Neuhaus and Soldati, 1999; Maniak, 2001; Rupper and Cardelli, 2001), revealing a striking degree of similarity to higher eukaryotes. After uptake and release of the cytoskeletal coat of actin and coronin, particles progress through the endolysosomal pathway. Phagosomes are rapidly acidified by delivery of proton pumps, and different sets of lysosomal enzymes are delivered (Souza *et al.*, 1997). Rab GTPases, clathrin, and dynamin are involved in various vesicle trafficking steps between endosomes and probably between contractile vacuoles and endosomes (for review, see Maniak, 1999; Neuhaus and Soldati, 1999). The function, structure, and dynamics of the pinocytic system have recently been described thoroughly (Neuhaus *et al.*, 2002), but equivalent work for the phagocytic pathway has not yet been performed with such precision. Recent evidence indicates that phagocytosis and macropinocytosis, although they are similar processes both involving PIP2, actin polymerization, RasS, coronin, Rab7, and myosins, are nevertheless biochemically distinct. The former is regulated by Rap1, RacC, and myosin VII, whereas the latter involves profilin, LmpA, and PKB (for review, see Cardelli, 2001).

Here, we present an initial molecular characterization of the successive membrane trafficking steps that occur during phagosome maturation in the model organism *D. discoideum*.

MATERIALS AND METHODS

Cell Culture

D. discoideum cells of wild-type strain Ax2 were grown axenically in HL5c medium (Sussman, 1987) on plastic dishes or in shaking culture (at 180 rpm) at 22°C.

Antibodies

The following antibodies were used: (1) a mouse monoclonal antibody (mAb) against a plasma membrane marker (PM4C4) (Neuhaus and Soldati, 2000); (2) a rabbit polyclonal antibody (pAb) against cathepsin D (CatD) (Journet *et al.*, 1999), (3) a rabbit pAb against the cysteine protease CP-p34 (these three antibodies were kind gifts from Dr. J. Garin, CEA, Grenoble, France); (4) rabbit pAbs against LmpA (Karakesisoglou *et al.*, 1999), LmpB, and LmpC (Janssen *et al.*, 2001); (5) rabbit pAbs against Rab7 (Laurent *et al.*, 1998) and against cytoplasmic fragments of Vti1 and VAMP7 (Bogdanovic *et al.*, 2002); and (6) mouse mAbs against coronin (de Hostos *et al.*, 1991), vacuolin A and B (221–1-1) (Rauchenberger *et al.*, 1997), PDI (221–135-1), calreticulin (Monnat *et al.*, 1997), and mitochondrial porin (Troll *et al.*, 1992). For Western blots, horseradish peroxidase (HRP)-coupled goat anti-mouse or anti-rabbit IgGs (Bio-Rad, Hercules, CA) were used at 1:5000 dilution; for immunofluorescence assay (IFA), goat anti-mouse or anti-rabbit IgGs coupled to Alexa 488 (Molecular Probes, Eugene, OR), Cy3 (Rockland, Gilbertsville, PA), and Cy5 (Rockland) were used at 1:2000 dilution.

Isolation of Phagosomes

The following buffers were used: Soerensen buffer (15 mM KH_2PO_4, 2 mM Na_2HPO_4, pH 6), homogenization buffer (20 mM HEPES-KOH, pH 7.2, 0.25 M sucrose, 1× Complete EDTA-free [protease inhibitor cocktail; Roche, Hertfordshire, UK]), membrane buffer (20 mM HEPES-KOH, pH 7.2, 20 mM KCl, 2.5 mM $MgCl_2$, 1 mM dithiothreitol [DTT], 20 mM NaCl), and storage buffer (25 mM HEPES-KOH, pH 7.2, 1.5 mM Mg-acetate, 1 mM $NaHCO_3$, 1 μM $CaCl_2$, 25 mM KCl, 1 mM ATP, 1 mM DTT, 1× Complete EDTA-free, 100 mM sucrose).

Phagosomes at different stages of maturation were obtained after feeding with latex beads (LBs) according to the following pulse-chase regime. Beads were adsorbed on cell surface simultaneously with plasma membrane biotinylation. For each sample, 10^9 cells were incubated with 2×10^{11} LBs of 0.8-μm diameter (Sigma, St. Louis, MO), first 5 min on ice in 5 ml Soerensen/120 mM sorbitol (Merck, Darmstadt, Germany), pH 8, containing 1 mg/ml Imuno-Pure NHS-LC-Biotin from Pierce (Rockford, IL) and then for 5 or 15 min in 100 ml HL5C medium at room temperature in shaking culture (120 rpm) at a concentration of 10^7 cells/ml. Phagocytosis was stopped by addition of 3 volumes of ice-cold Soerensen/sorbitol followed by centrifugation. Sorbitol (120 mM) prevented abrupt changes in osmotic conditions and increased buffer density to reduce sedimentation of noningested beads. This step was repeated once. The cell pellet was resuspended in a small volume of ice-cold medium, and the chase was started by adding the suspension into 100 ml of medium at room temperature for 15–165 min. Chase was stopped as mentioned for the pulse, including the washing step. Phagosomes were isolated according to Desjardins *et al.* (1994b), with some modifications. Cells were homogenized by eight passages through a ball homogenizer (EMBL, Heidelberg, Germany) with a void clearance of 5 μm. The homogenate was incubated with 10 mM Mg-ATP (Sigma) for 15 min on ice before loading onto sucrose step gradients. Alternatively, cells were incubated before homogenization with 5 μM latrunculin B (Alexis, San Diego, CA)

for 5 min at room temperature. Gradients were centrifuged for 3 h at 100,000 × *g* in a Beckmann SW 28 rotor. The interface of 10 and 25% sucrose was collected, diluted in ~30 ml of membrane buffer, and centrifuged for 1 h at 100,000 × *g* in the same rotor. The pellet was resuspended in storage buffer and stored at −80°C or partly mixed with Laemmli buffer for SDS-PAGE (Laemmli, 1970). To normalize phagosome concentrations between different samples, the volumes of storage and Laemmli buffer were adjusted by measuring the number of LBs trapped in phagosomes by measuring light-scattering at 600 nm.

Quantitative Immunoblotting

After SDS-PAGE (Laemmli, 1970) and transfer onto nitrocellulose membrane (Protran, Schleicher & Schuell, Dassel, Germany), quantitative immunodetection was performed as described (Schwarz *et al.*, 2000) using ECL plus (Amersham) and a chemiluminescence imager (LAS-1000, Fuji Film, Tokyo, Japan). Data quantification was carried out with Image Gauge version 3.0 (Fuji Film).

Two-dimensional Gel Electrophoresis

Extracts were prepared as follows. Whole cells, a crude membrane fraction (obtained as the particulate material of a postnuclear supernatant) and LB phagosome samples were solubilized in lysis buffer containing 7 M urea (Merck), 2 M thiourea (Merck), 2% wt/vol CHAPS (Sigma Aldrich, St. Louis, MO, USA), 1% wt/vol DTT (Sigma), 2% vol/vol Pharmalyte pH 3–10 (Amersham Pharmacia Biotech, Uppsala, Sweden), and a protease inhibitor cocktail (Complete EDTA-free, Roche) (Rabilloud *et al.*, 1997; Gorg *et al.*, 2000). Suspensions were sonicated 3 × 10 min at 4°C in a bath sonicator, incubated at room temperature for 2 h, and centrifuged (60 min, 75,000 × *g*) in a Beckmann TL 120 (Palo Alto, CA) except for the LB phagosome samples. Supernatants and whole samples were stored at −80°C until further use. Electrophoresis was carried out as follows: Extracts were separated in the first dimension using 18-cm strips with immobilized nonlinear pH 3–10 gradients according to the manufacturer (Amersham), followed by standard SDS-PAGE as described (Gorg *et al.*, 2000; Regula *et al.*, 2000), with minor modifications. In brief, samples were applied using in-gel reswelling and focused for 16 h on an IPGphor (Amersham). Then, strips were equilibrated first in a solution containing DTT and then with iodoacetamide (Sigma). Two-dimensional gels were stained with either silver (Rabilloud *et al.*, 1988) or colloidal Coomassie blue (Novex, San Diego, CA) according to the manufacturer's instructions.

Protein Sequencing

In-gel digestion was performed as described (Rosenfeld *et al.*, 1992; Shevchenko *et al.*, 1996), with minor modifications. Briefly, excised gel plugs were washed with 100 μl water, 100 μl 50% acetonitrile and were subsequently shrunk in 100 μl acetonitrile. Modified trypsin (Promega, Madison, WI) (12 ng/μl) in 40 mM ammonium bicarbonate buffer was added and incubated overnight at 37°C. Custom-made chromatographic columns were used for desalting the supernatant of the tryptic digest. A column consisting of 20 μg Poros R2 material (50 μm bead size, PerSeptive Biosystems) in 5 μl 75% methanol/1% acetic acid was packed in a constricted GELoader tip (Eppendorf). After equilibration with 1% acetic acid, the sample was loaded, the column was washed with 20 μl 1% acetic acid, and peptides were eluted with 1 μl 75% methanol/1% acetic acid directly into a precoated borosilicate nanoelectrospray needle (MDS Protana, Odense, Denmark). Mass spectrometry (MS) analysis was performed on a quantitative time-of-flight mass spectrometer (PE SIEX, Weiterstadt, Germany) equipped with a nano-electrospray ionization (ESI) ion source (MDS Protana, Odense, Denmark). A potential of 900 V was applied to the nano-electrospray needle. Declustering potential and focusing potential were set to 40 and 100, respectively. Fragmentation of selected peptides (unit resolution) was usually performed by three different collision energies (22, 27, and 35 V). Data were processed using Bioanalyst software (PE SIEX).

Lipid Analysis

Lipid extracts of a crude membrane fraction or phagosome samples were prepared as described by Bligh and Dyer (1959). They were dried under a stream of nitrogen and redissolved in a small volume (20–200 μl) of methanol/chloroform (2:1) containing either 10 mM ammonium acetate (added from a 100-mM stock solution in methanol) for positive ion analyses or no additive for negative ion measurements. Total phospholipid content of samples was measured by the method of Rouser *et al.* (1970). The lipid extracts were analyzed by nano-ESI tandem MS as described previously (Brügger *et al.*, 1997), including positive ion scans specific for phosphatidylserines, phosphatidylcholines (PCs), and phosphatidylethanolamines (PEs).

Electron Microscopy

Phagosomes were incubated in 100 mM cacodylate buffer overnight. After 20 min in 4% osmium tetroxide/200 mM cacodylate buffer, a standard procedure for dehydration followed. Infiltration of intermedium was done by increasing the amount of epoxy resin in 1,2-propylene oxide before embedding in Araldit CY212 (Agar Scientific). Ultrathin sections of 80 nm were contrasted in 2% uranyl acetate in methanol and lead citrate and viewed in a Philips EM 400T.

Immunofluorescence Microscopy

Cells were plated on grade 0 coverslips, fixed by plunging in −85°C methanol, stained, and mounted in ProLong Anti-Fade (Molecular Probes) as described (Neuhaus *et al.*, 1998; Neuhaus and Soldati, 2000). Fluorescence-labeled LBs of 1-μm diameter and TRITC-labeled yeast were used as follows. Medium in 6-cm Petri dishes was replaced by medium with an LB or a yeast suspension, respectively. Cells were allowed to ingest the particles for 5 or 15 min before excess beads or yeasts were washed away by several changes of medium. The same time course of chasing was used as for purification of LB phagosomes. Observations were performed with Leica confocal microscopes TCS-NT or SP2, with a 63× oil 1.4-NA objective. Images were imported into Adobe Photoshop (Adobe Systems) or NIH Image (National Institutes of Health, Bethesda, MD) for processing.

Quantitative analysis of the presence of CatD in maturing phagosomes was performed as follows. From each time point of phagocytosis of TRITC-labeled yeasts, single optical sections of fields of cells stained for CatD and vacuolin were recorded and printed out; their order was randomized, and they were scored in a blind manner. In total, 2448 phagosomes were counted and evaluated as described in the legend to Figure 6.

RESULTS

Establishment and Improvement of a Phagosome Preparation in D. discoideum

As a first step in our in-depth investigation of the mechanisms of phagosome formation and maturation, we adapted the LB phagosome purification from Desjardins and colleagues (Desjardins *et al.*, 1994a; Garin *et al.*, 2001) to *D. discoideum*. Preliminary experiments of phagosome isolation failed to show the expected high purity, because PDI, a marker for endoplasmic reticulum (ER), and the mitochondrial porin were clearly detectable (Figure 1, B and C). In

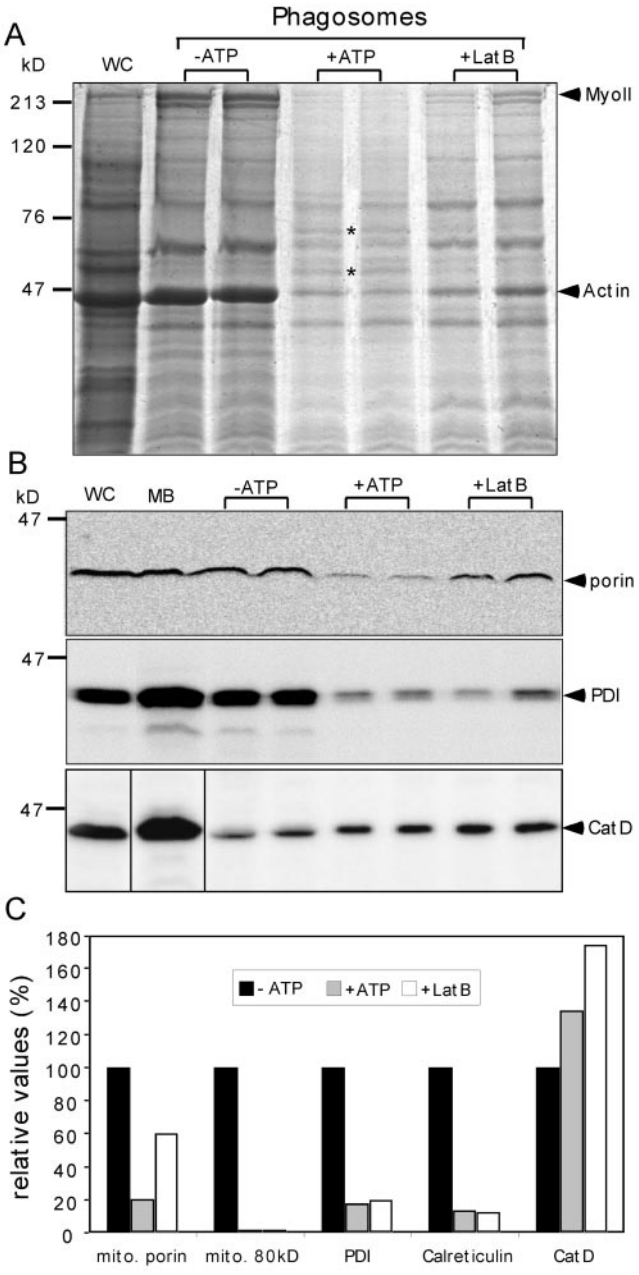

Figure 1. Improvement of LB phagosome purification. (A) Coomassie-stained gel of phagosomes obtained after 15 min of pulse feeding. Phagosomes were purified in the absence (−ATP) or presence (+ATP) of ATP or latrunculin B (LatB). The lanes are loaded with the same numbers of LB phagosomes, normalized by measuring light-scattering at 600 nm. Myosin II (MyoII) and actin are major contaminants in absence of ATP. Other ATP-dependent bands are marked by dots and discussed in the text. (B) The abundance of contaminating mitochondrial porin, protein disulfide isomerase (PDI), and CatD was visualized by Western blot analysis of fractions presented in (A) and quantified (C). As for experiments presented in subsequent figures, quantifications were carried on 2–3 independent experiments from digitally recorded data. Representative examples are shown. The sizes of molecular-weight markers are indicated on the side of the gel. WC, whole cell extract; MB, crude membrane extract.

addition, we observed that the sucrose gradients needed significantly longer centrifugation times to reach equilibrium, and finally, the 25% sucrose step of the gradients contained flocculated material. Coomassie-stained gels of phagosomal fractions obtained after 15 min of pulse feeding (Figure 1A) showed abundant coenrichment of actin and myosin II. We reasoned that excessive formation of a dense meshwork of cytoskeletal proteins (mainly of actin and myosin II, because the levels of tubulin were very low) around the phagosomes might entrap contaminating organelles. Therefore, we tested whether addition of 10 mM ATP or 5 μM of latrunculin B decreased the artifactual interactions of phagosomes with a rigor mortis actomyosin meshwork. The addition of ATP or of latrunculin B resulted in a macroscopically visible difference. The clumps of membrane material disappeared, leaving a homogeneous suspension of phagosomes. Coomassie staining (Figure 1A) showed that addition of ATP resulted in almost complete reduction of actin and myosin II and disclosed a more distinct band pattern, whereas latrunculin B led to intermediate and less reproducible results. Note that whereas all the phagosomal samples were normalized for LB content by measuring light scattering, the whole-cell and crude membrane extract lanes (Figures 1, 4, 5, and 7) were loaded with a standard but arbitrary amount of protein corresponding to ~5- to 10-fold more than in the phagosome sample lanes. This allows comparison between experiments, but the signal intensities thus do not directly reflect the enrichment or depletion of the markers analyzed. In contrast to actin and myosin, a majority of bands remained at comparable intensity in the different samples. Interestingly, a few proteins were even slightly more abundant after ATP treatment (Figure 1A, asterisks). These two bands were excised and identified by MS as a DnaJ-tetratricopeptide repeat–containing protein of 60 kDa and Ddj1, a 45-kDa heat shock protein. Western blot detection confirmed that contamination could be significantly reduced by ATP and to a lesser extent by latrunculin B (Figure 1B). Quantification showed that both ER markers and the mitochondrial porin were reduced at least fivefold and that another uncharacterized mitochondrial protein of 80 kDa was no longer detectable (Figure 1C). The samples treated with latrunculin B showed a similar but intermediate behavior. Importantly, as the level of contamination was reduced, the specific activity of CatD increased, leading to an overall average 10-fold improvement in yield and purity.

The quality of the phagosome preparation was also controlled by electron microscopy. As shown in Figure 2, a tightly wrapped membrane surrounded the majority of LBs. A few phagosomes containing other membranous particles were also present (not shown). Most beads were found in single-bead phagosomes, but phagosomes with 2–5 beads were also seen (Figure 2C, arrowhead), a positive indication for the gentle preparation. Some membrane whirls were seen that probably had peeled off the ingested beads during fixation. No intact mitochondria and little ER debris dotted with ribosomes were observed, illustrating the very low levels of contamination determined by Western blotting. Finally, some vacuoles were reminiscent of autophagosomes, with cytosol-like components inside (Figure 2B, arrowheads). Because of the simplicity and gentleness of treatment, ATP was used further, allowing generation of a highly purified phagosome fraction with excellent yields. The sig-

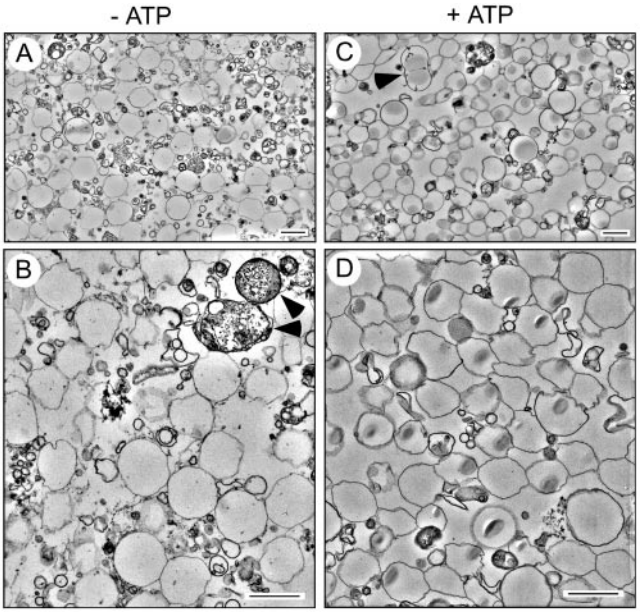

Figure 2. Electron microscopic analysis of phagosomal membranes. Cells were fed for one hour with LBs, and LB phagosomes were purified in the absence (A and B, −ATP) or presence (C and D, +ATP) of ATP by sucrose gradient centrifugation. Low (A and C) and high (B and D) magnifications of the fractions are shown.

nificance of the ATP-dependent association of some proteins is as yet unclear and will require additional investigation.

Preliminary Characterization of Protein and Lipid Content of Phagosomal Samples

To document the feasibility of applying comprehensive proteomic and lipidomic approaches to phagosomes, overall protein and lipid contents were analyzed. Proteins of a crude membrane extract obtained from a postnuclear supernatant (Figure 3A) and of an early phagosome sample (Figure 3B) were fractionated by two-dimensional gel electrophoresis and silver-stained. Confirming the specificity and purity of the phagosome samples, the protein patterns were extremely distinct, rendering it difficult to mark identical spots on both gels. Some of the major spots from the phagosome gel (Figure 3B) were excised and identified by tandem MS. It showed that even at early time points, the vacuolar ATPase was present and most of its subunits were identifiable. The analysis also revealed the presence of expected endosomal markers, such as coronin and vacuolin A and B. These markers showed a spectacular enrichment (at least 10-fold to 50-fold) compared with the crude membrane fraction, and it will be extremely informative to complete this proteomic analysis to possibly discovery new specific phagosomal components.

In parallel, lipids were extracted from the same membrane and phagosome fractions and analyzed by nano-ESI tandem MS. As an illustration of the principle, one example of a PE-specific scan is shown for both fractions (Figure 3, C and D), but the overall picture and conclusions reached were similar for positive and for negative ion measurements, and in particular for the PC- and phosphatidylserine-specific scans. In the crude postnuclear membrane fraction, PE with acyl chains totaling 36 carbons and 2 unsaturations were the predominant species, and the lyso-PEs were present in low quantities (Figure 3C). The major differences in the early phagosomes (and true also for PC) were the significant increase of lyso-PE and also the shift toward PE with shorter acyl chains with fewer unsaturations (Figure 3D). In conclusion, the system now established offers a unique opportunity to obtain a comprehensive and parallel cartography of endosomal proteins and lipids with any desired temporal resolution, from uptake to the final phase of secretion.

Plasma Membrane Proteins Are Recycled from Maturing Phagosomes with Distinct Kinetics

Preliminary pulse-chase studies monitored by live microscopy, immunofluorescence (Figure 6) and immunoblotting (Figure 5) showed that time points as early as 5 min and spread over the next 3 h gave a good overview of phagosome maturation, from uptake until egestion of undigested remnants via different membrane trafficking phases. To follow trafficking of plasma membrane proteins and their potential recycling from the maturing phagosome, the cell surface was biotinylated right before the feeding pulse with LBs was begun. Previous experiments showed that surface biotinylation of membrane proteins serves as a faithful marker of membrane uptake and recycling, because little or no degradation was measured during the time of the experiment (Neuhaus and Soldati, 2000). As revealed by streptavidin-HRP blot staining, the pattern of labeled proteins in early phagosomes (Figure 4A, 5′/0′) was similar to the one obtained after cell surface labeling at 0°C (Figure 4A, BiotWC), with two exceptions. The major band at 80 kDa (Figure 4A, *) is an endogenously biotinylated protein that is quantitatively absent from phagosomes, and the major band in early phagosomes (Figure 4A, arrowhead at 30) is barely detectable in the plasma membrane–labeled proteins. The prominent band at 130 kDa corresponds to gp130 (Chia, 1996), a glycoprotein shown to recycle to the plasma membrane from an early endosomal compartment of the macropinocytic pathway (Neuhaus and Soldati, 2000). Most strikingly, as revealed by digital quantification (Figure 4C), the overall intensity of labeling dropped ~20-fold between the 5′/0′ and the 15′/2h45′ time points, with a major 50% drop between 15′/15′ and 15′/45′. Analysis of individual bands revealed a more complex picture (Figure 4, A and C). Whereas a protein of 40 kDa was removed from phagosomes with a kinetics faster than average, another of 30 kDa followed the average kinetics, and gp130 increased during the first 15 min of chase before being abruptly retrieved between 15′/15′ and 15′/45′. In addition, whereas both the 30- and 40-kDa proteins were quantitatively recycled (>90%) before egestion, gp130 declined only to ~20% of its original intensity. The time-dependent profile of PM4C4, a plasma membrane marker used to trace the macropinocytic pathway and shown to accumulate in endosomes of MyoA−/B− cells (Neuhaus and Soldati, 2000), was monitored (Figure 4B). Contrary to the bulk of plasma membrane components but somewhat similarly to gp130, PM4C4 first accumulated transiently up to the 15′/15′ time point before being retrieved to reach a similar concentration in late as in early phagosomes. We conclude that retrieval of plasma

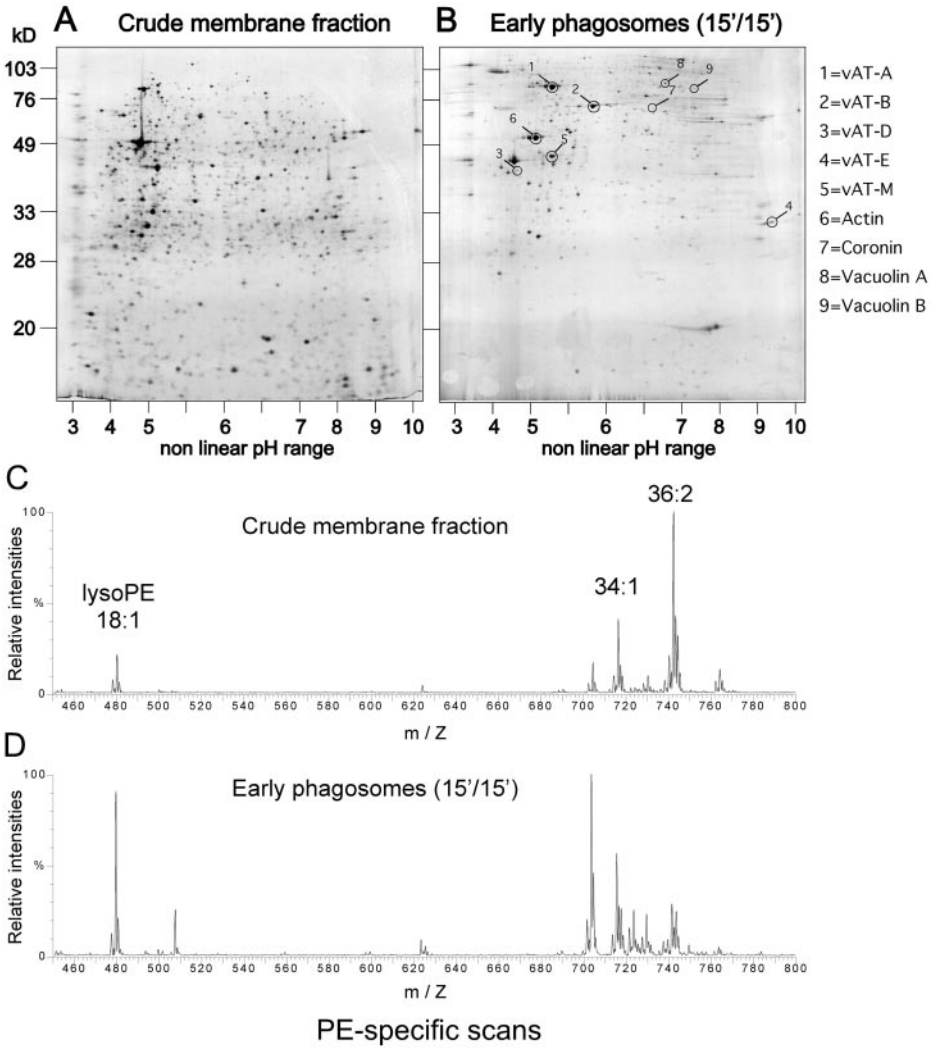

Figure 3. Comparison of protein and lipid profiles from phagosomes and a crude membrane fraction. (A and B) Two-dimensional gel analysis of a crude membrane fraction (A) from which the LB phagosomes were purified. Cells were fed with LBs for 15 min and chased for 15 min (15′/15′) before homogenization and purification of early phagosomes (B). Proteins were visualized by silver staining. Spots marked and numbered in (B) were identified by MS. (C and D) After extraction, lipids were analyzed by ESI-MS/MS. The same fractions as in A and B were analyzed. Only part of the whole mass-to-charge (m/Z) spectrum of PE-specific scans is shown. Identity of three major species is indicated above the traces.

membrane components is operated by distinct, specific membrane trafficking steps but that overall recycling efficiency is extremely high and comparable to the one reached in mammalian cells.

Specific Changes in Protein Composition Accompany Phagosome Maturation

As indicated by 2D gel analysis, the composition of phagosomes represents a specific subset of total cellular proteins. To monitor time-dependent changes in their composition, we started an analysis by SDS-PAGE, protein staining, and immunoblotting for known endosomal markers. Coomassie staining revealed that whereas many proteins were present throughout phagosome maturation at a relatively constant level (Figure 5A, arrowheads), some were present only during brief phases (Figure 5A, circles and diamonds). A doublet of proteins was clearly distinguishable only before chase (Figure 5A, 5′/0′ and 15′/0′, circles); two doublets of high-molecular-weight proteins were present mainly at the earliest time point (Figure 5A, 5′/0′, diamonds); a 40- and a 100-kDa protein were specific of the 15′/45′ and 15′/2h45′ time points, respectively (diamonds). Identification of these proteins is a focus of ongoing research.

Some Lysosomal Proteins Are Selectively Delivered and Retrieved from Maturing Phagosomes

The next step was to unveil the particular temporal dynamics of some phagosomal constituents. First, we investigated the profile of hydrolases such as CatD, the *D. discoideum* homologue of a mammalian endoprotease, and CP-p34, a member of the cysteine protease family (Figure 5B). Both CatD and CP-p34 were barely detectable at the earliest time point, 5′/0′, and increased with similar kinetics, fivefold and threefold, respectively, at the 15′/0′ time point, and 20-fold and 12-fold, respectively, at the 15′/15′ time point. During later phagosome maturation, the fates of the two hydrolases were markedly different. CatD continued to increase and reached a nearly 50-fold enrichment at 15′/1h45′ before decreasing slightly at the latest time point. In contrast, CP-p34 was retrieved earlier, first decreasing slowly, followed

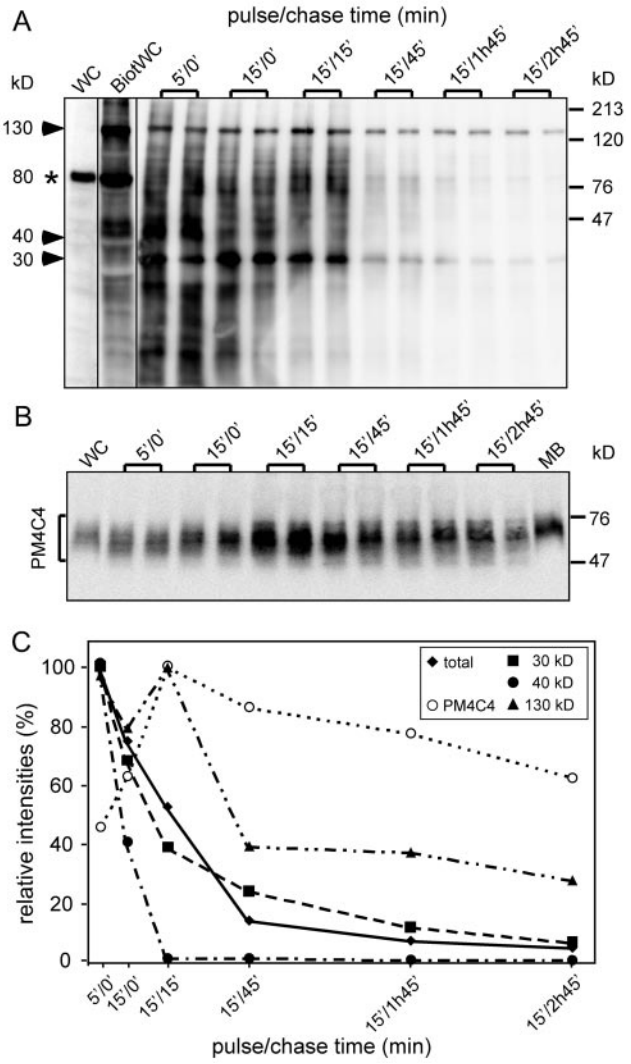

Figure 4. Recycling of plasma membrane components is operated in distinct steps. Before uptake of LBs, cell surface proteins were labeled with a biotinylated cross-linker. Extracts and purified phagosomes were separated by SDS-PAGE and blotted onto a membrane. Detection was carried out by avidin-HRP (A). In whole-cell extracts of nonbiotinylated cells (WC), very low background is visible, except an endogenously biotinylated 80-kDa protein (asterisk). After biotinylation, dozens of bands appear, with a particularly prominent one at 130 kDa. (B) The blot was then stripped and probed with an antibody against a plasma membrane glycoprotein (PM4C4). Signals were quantified by chemiluminescence imager, and the average of doublets was plotted as a function of the pulse/chase time (C). Total indicates that the signal was integrated over the whole lane, and 30 kDa, 40 kDa, and 130 kDa indicate three major biotinylated bands that behaved with distinct kinetics.

by a drop to ~20% of its maximum between 15′/1h45′ and 15′/2h45′. These features are best visualized in the corresponding graph (Figure 5D).

Lysosomal glycoproteins of the ubiquitous CD36/LIMPII family have recently been described in *D. discoideum* (Janssen *et al.*, 2001). They are highly glycosylated, share a similar membrane topology, and probably are present in different subsets of storage lysosomes. Our temporal profiling (Figure 5, B and C) revealed that LmpA and LmpC apparently trafficked with nearly identical kinetics. LmpA rose constantly to an approximately eightfold increase from the 5′/0′ time-point to 15′/45′ before it reached a plateau and finally decreased ~25% at 15′/2h45′. In sharp contrast, LmpB was present in the very early phagosomes and was rapidly retrieved with a kinetics similar to that observed previously for plasma membrane components (Figure 4), decreasing >50% between 15′/15′ and 15′/45′. This low level of LmpB was maintained to the end.

To compare our kinetic results with knowledge accumulated in other laboratories, we used a series of reference markers, two of which are shown in Figure 5D. Coronin was shown to associate with nascent phagosomes and to disappear after a few minutes, concomitantly with the actin coat. It is also present transiently on late phagosomes and secretory lysosomes, being gradually replaced by vacuolin, which accompanies these compartments during egestion and was also reported at the plasma membrane. The profiles of coronin and vacuolin (Figure 5D) corroborate these earlier findings perfectly and extend them in a more quantitative manner. In addition, for the first time, we detected vacuolin on nascent phagosomes.

Direct Visualization of the Delivery and Recycling of CatD in Model and Natural Phagosomes

To directly visualize the kinetics of trafficking to and from the maturing phagosome obtained by the quantitative biochemical approach, cells were fed with fluorescence-labeled LBs in a pulse-chase regimen equivalent to the one used for phagosome purification (Figure 6, A and C). In addition, to establish a correlation with a more physiological particle, cells were fed in parallel with TRITC-labeled yeasts (Figure 6, B and D). After fixation by rapid freezing, cells were double-stained for CatD and PM4C4 (Figure 6, A and B), because CatD showed a very distinct kinetics of accumulation and late recycling. PM4C4, a plasma membrane marker, was used to determine whether beads and yeast were completely ingested. At early time points, a typical punctate lysosomal distribution of CatD was observed (Figure 6, A and B, 5′/0′, arrowheads), with occasionally a larger ring-like structure (not shown), probably similar to the "ring of dots" positive for lysosomal markers circling organelles of the macropinocytic pathway (Neuhaus *et al.*, 2002). As soon as a particle was engulfed, lysosomes appeared to clump (Figure 6, A and B, 15′/0′ and 15′/15′, arrowheads) and associated with phagosomes (Figure 6, A and B, 15′/0′ and 15′/15′, arrows). Between 15′/15′ and 15′/1h45′, most of the yeast phagosomes had a yellowish appearance because of the overlay of the green-labeled CatD diffusing inside the porous red-labeled yeasts (Figure 6B, black asterisks), but from 15′/45′ onward and with increasing frequency, more reddish yeasts were again visible, surrounded by CatD dots (Figure 6B, 15′/45′ and 15′/1h45′, arrows). Yeasts that were egested were red again, demonstrating the quantitative retrieval of CatD before exocytosis (Figure 6B, 15′/45′, white asterisk). The same was true for the model LB phagosomes, with the difference that CatD could not diffuse inside the beads and instead formed a rim of staining around the bead (Figure 6A, 15′/1h45′ and 15′/2h45′, arrows and insets).

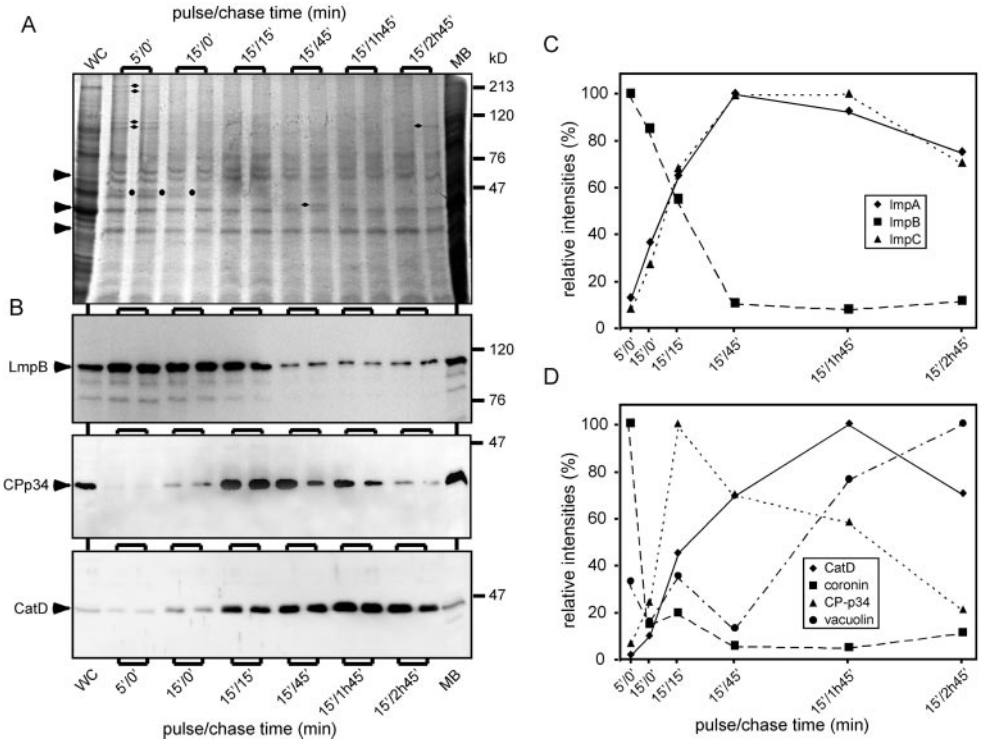

Figure 5. Detailed kinetic analysis of phagosomal components revealed distinct membrane trafficking steps. (A) Phagosomal fractions obtained at different pulse/chase feeding regimens with LBs were separated by SDS-PAGE and either stained with Coomassie blue (A) or blotted onto a membrane and analyzed by immunoblotting (B). The intensity of the bands marked by arrowheads was almost constant, whereas bands marked by other symbols were present during a brief period (circles) or even at a single time point (diamonds). (B) Quantitative immunoblotting revealed significantly distinct phases in the life of a phagosome. (C) The behavior of LmpB is not representative of other members of the family. (D) Coronin is a marker of early phagosomes and, together with vacuolin, of late secretory phagosomes.

To precisely define the stage at which retrieval of CatD occurred, double staining of CatD and vacuolin was performed (Figure 6, C and D). At early time points, vacuolin-positive compartments were observed (Figure 6, C and D, 15′/0′, arrows) and represent secretory lysosomes of the pinocytic pathway (Rauchenberger *et al.*, 1997; Jenne *et al.*, 1998; Neuhaus *et al.*, 2002). Despite detection on purified phagosomes (Figures 3B and 5D), vacuolin was not visualized by immunofluorescence associated with nascent and early phagosomes. As described above, right before egestion, yeasts were circled by an increasingly distinct vacuolin-positive ring and were red again (Figure 6, C and D, 15′/2h45′, arrowheads). During this late maturation step, dots of CatD were intermingled with the vacuolin ring. Note that at any given point in this later phase, on average, only ~10 to 20% of the phagosomes were involved in final maturation and recycling. To strengthen the argument, we quantified the presence of CatD. Approximately 2500 phagosomes containing no (red), intermediate (intermediate), and highest (yellow) levels of CatD were scored, and the proportions of each category were represented as a function of time (Figure 6E). The disappearance of early, CatD-negative phagosomes correlated with the rise in phagosomes with intermediate levels, whereas the proportion of phagosomes containing the highest levels was lagging, indicative of a precursor–product relationship. Concomitantly with retrieval of CatD at 15′/2h45′, the proportion of CatD-negative phagosomes increased again. In conclusion, the major phase of CatD recycling from maturing phagosomes, contrary to the earlier retrieval phase of CP-p34, appears to coincide with the last remodeling before egestion, concomitantly with recruitment of vacuolin. In addition, the functional mechanisms of membrane trafficking studied appear to occur with indistinguishable kinetics in natural and model phagosomes.

Components of the SNARE Machinery Accompany Trafficking of Cargos to and from Phagosomes

Components of the SNARE machinery and its regulatory factors have recently been described in *D. discoideum*. In addition to the ubiquitous NSF and SNAPs, endosomal SNAREs have been identified, among them the t-SNARE component Vti1 and the v-SNARE Vamp7. Vti1 is associated with Syntaxin7 (Bogdanovic *et al.*, 2002). Syntaxin 7 and Rab7 have been involved in endosome maturation and homotypic fusion (Buczynski *et al.*, 1997; Laurent *et al.*, 1998; Bogdanovic *et al.*, 2000). The exact role of Vti1 in *D. discoideum* is not yet known. The temporal profile of these proteins was monitored by quantitative immunoblotting and revealed that Rab7 and Vti1 followed very similar kinetics of association and retrieval from the maturing phagosomes, whereas Vamp7 had a distinct fate (Figure 7, A and B). Both Vti1 and Rab7 were present very early and followed a pattern resembling that of PM4C4 (Figure 4C). Vamp 7 accumulated more slowly, reached a peak at approximately 15′/45′, and was retrieved almost quantitatively before egestion. Even more interestingly, delivery and retrieval of these endosomal SNAREs correlated with trafficking of specific cargo molecules (Figure 7B). The delivery of LmpA coincided with accumulation of both Rab7 and Vti1 and its recycling to the kinetics of Vamp7 retrieval. In contrast, delivery of CP-p34 was closer to the profile of Rab7 and Vti1 accumulation, but its recycling paralleled the decrease of Vamp7. In conclusion, our system has the power to precisely

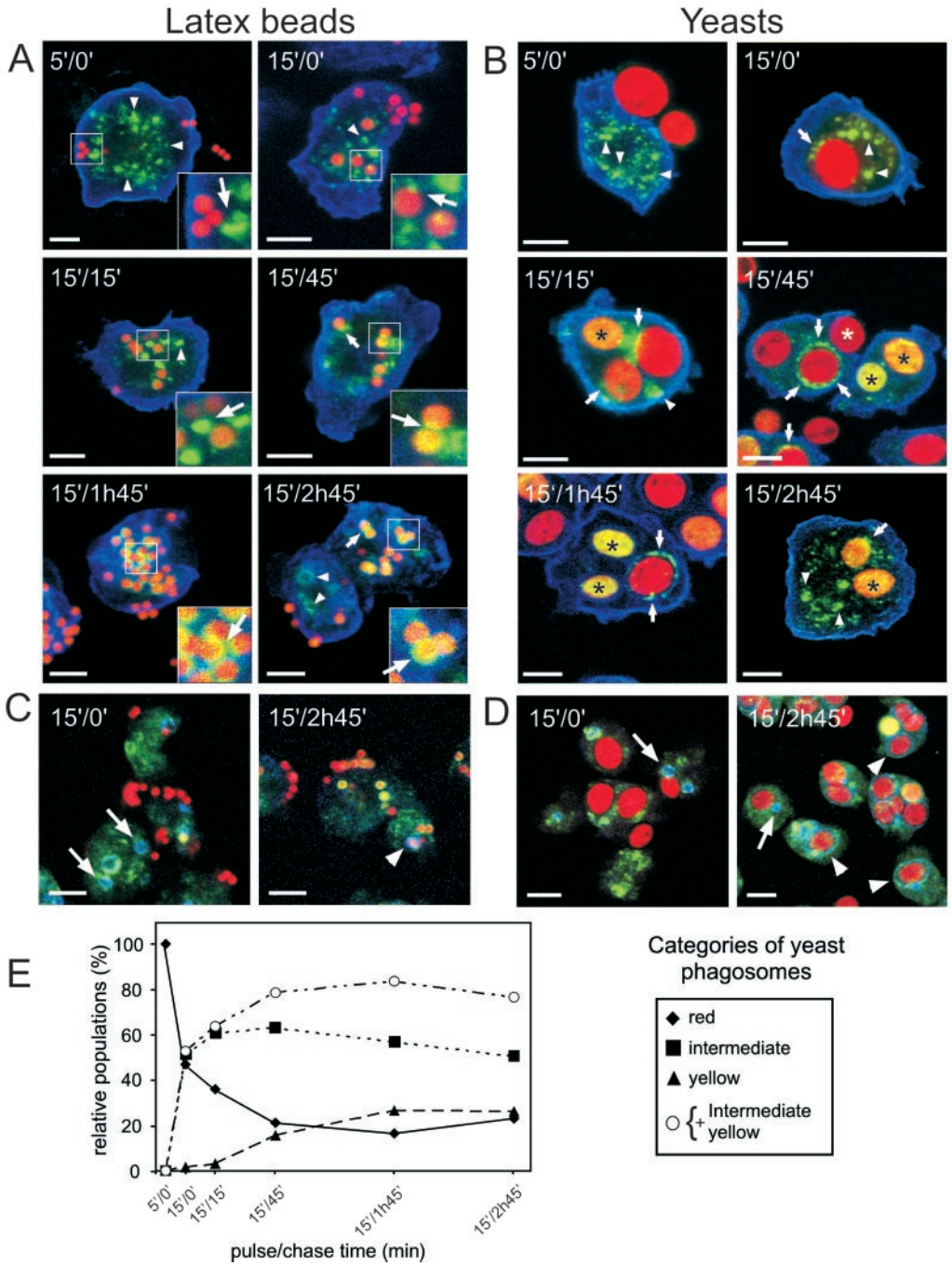

Figure 6. Visualization of delivery of CatD to maturing phagosomes and of its recycling before egestion. Cells were fed with either fluorescent LBs (red in A and C) or TRITC-labeled yeasts (red in B and D) according to the same pulse/chase regime as used for the purification. Cells were fixed and stained for CatD (green in A to D) and the plasma membrane marker PM4C4 (blue in A and B) or the secretory lysosome marker vacuolin (blue in C and D). During and shortly after uptake, the LBs and yeasts appeared red. Because of overlay of red and green, delivery of CatD colored (or circled) the particles yellow (black asterisks). After quantitative removal of CatD before egestion, the particles were red again (white asterisk). CatD was first present in small punctate lysosomes (arrowheads in A and B) that associated with the phagosome (arrows in A and B) either during the delivery (early time points) or removal of CatD (later time points). At early time points of phagocytosis, vacuolin was associated only with late secretory lysosomes (arrows in C and D) but was then recruited onto late phagosomes (arrowheads in C and D). At late time points, vacuolin-positive phagosomes were red again, showing that CatD had been removed right before egestion. (E) Presence of CatD was quantified in 2500 maturing phagosomes and attributed to one of the following categories: red for phagosomes that did not contain measurable level of CatD, yellow for phagosomes containing the highest levels of CatD, and intermediate for phagosomes containing either a homogeneous submaximal level of CatD and/or CatD in the form of punctate structures. The data are presented as a proportion of each category at every time point. Bars, 5 μm.

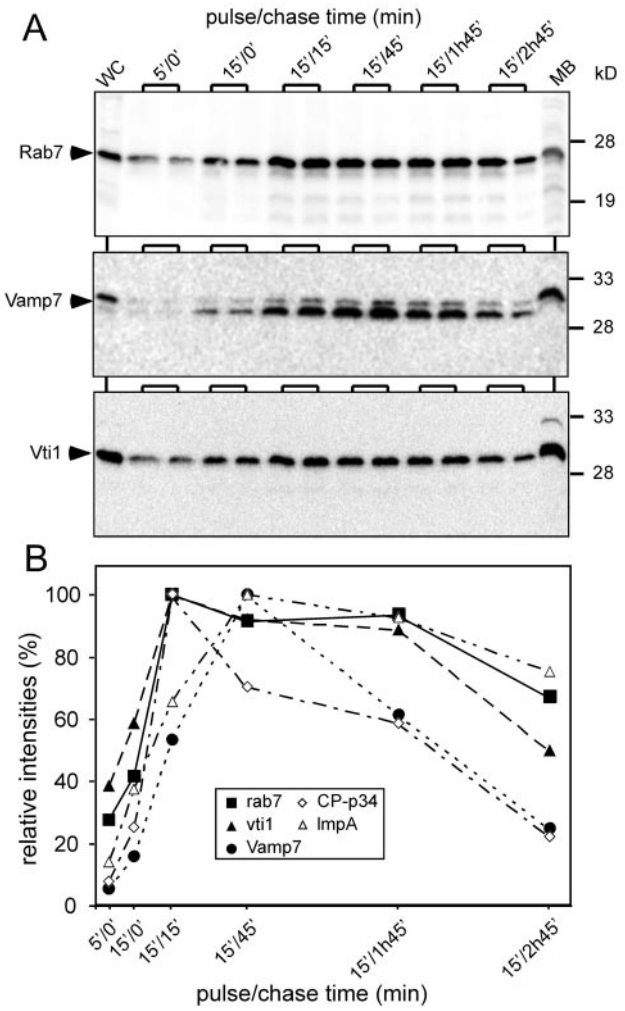

Figure 7. The trafficking of specific cargoes is accompanied by appearance and disappearance of endosomal SNARE components. Phagosomal fractions were analyzed with antibodies directed against components of the SNARE machinery, Rab7, Vti1, and Vamp7 (A), using quantitative immunoblotting (B). The traces are superimposed with those of two cargos, CP-p34 and LmpA (from Figure 5).

monitor trafficking of SNARE proteins that determine the transport of specific cargos during each phase of phagosome maturation.

DISCUSSION

Establishment and further development of a phagosome purification protocol in a genetically and biochemically tractable organism such as *D. discoideum* is a decisive step toward a comprehensive investigation of the cellular and molecular mechanisms of phagocytosis. As documented by biochemical techniques and electron microscopy, this gentle and efficient protocol allows purification of phagosomes at every stage of their complex maturation to preserve their integrity and to avoid the piggybacking of contaminating organelles through formation of a rigor mortis meshwork of F-actin and myosins. Then, the synergistic combination of rapid-freezing immunofluorescence methods and biochemical characterization offers a unique opportunity to establish a precise fingerprint of each stage of phagosome maturation with unrivaled spatial and temporal resolutions.

Here, in an initial molecular characterization, we have applied immunocytochemical tools to reveal trafficking of SNARE components and cargo molecules, their delivery to the phagosome, and their retrieval before egestion, as well as association with cytosolic components. Our investigations also integrate data from immunoblotting on purified phagosomes and immunofluorescence on rapidly frozen cells. As revealed for CatD, we observe excellent correspondence between the temporal profiles of markers delivered to and retrieved from maturing phagosome using both methods. In addition, despite recent findings that indicate differences in the fate of a phagosome depending on the mechanical properties of the particle (Beningo and Wang, 2002), here, use of yeast particles emphasized that our findings based on the model LB phagosome are generally valid. Furthermore, whereas blotting obviously analyzes a population of phagosomes, immunofluorescence follows the fate of individual organelles. This not only proved to be complementary to the biochemistry but also greatly extended our understanding of recycling of phagosomal components before egestion (see detailed discussion below). It is important to note that this final step of phagocytosis in *D. discoideum* was long considered a peculiarity of the system, but recent findings now establish its conservation in macrophages as well (Di *et al.*, 2002).

Temporal profiling of a large number of markers indicated at least three major incoming and three outcoming membrane trafficking phases accompanying phagosome maturation. Molecular investigation of these membrane trafficking steps has just started, but correlation between transport of cargos and presence of SNARE components presents us with a solid and comprehensive working model. The following scenario recapitulates our findings and evidence accumulated in other labs. The nascent phagosome is associated with coronin, which, together with actin, is rapidly shed as the V-ATPase is delivered to acidify its content (Maniak, 1999, 2001). For the first time, we observed that vacuolin was detectable on nascent phagosomes, which might reflect its presence at the plasma membrane after exocytosis of the secretory lysosomes/phagosomes (Rauchenberger *et al.*, 1997). The mAb used does not discriminate between vacuolin A and B, but both are present on phagosomes as identified by two-dimensional gel and MS. LmpB was delivered with kinetics similar to those of the V-ATPase and was most abundant at the earliest time point measured, although both are undetectable at the plasma membrane by immunofluorescence (our unpublished observations). Delivered in a second trafficking step, some hydrolases such as CP-p34 start accumulating, whereas some like CatD are delivered at even later time points. There are also three retrieval phases. One is followed by LmpB and most plasma membrane markers; it is a steady and sharp decrease started at 5′/0′ and finished by the 15′/45′ time point. A second phase, best visualized by the decrease in CP-p34, occurred primarily between 15′/15′ and 15′/1h45′. The third phase occurs concomitantly with the preparation for exocytosis and is probably less

specific because of the obvious need to efficiently retrieve all lysosomal and phagosomal components to avoid their secretion or insertion at the plasma membrane.

Because beads were adsorbed onto cells on ice before shock warm-up and because sharp kinetic profiles were monitored, we conclude that our protocol gives access to a synchronized wave of phagosomes, the majority of which proceeds in a precise temporal order through the first steps of maturation. Nevertheless, because the analysis averages $\sim 10^{10}$ phagosomes per time point, this does not preclude that a minority of phagosomes mature at different rates and that some might acquire a distinct subset of proteins. Quantitative analysis of CatD trafficking revealed that the proportion of phagosomes with highest CatD concentration increased only after the one with intermediate levels, indicating a precursor–product relationship. In any case, it appears inherent to phagosome (and endolysosome) physiology that, at any given time, only 10–20% of late phagosomes are engaged in the last recycling step before egestion. This asynchrony, perfectly visualized by immunofluorescence microscopy, explains the relatively small drop in CatD between the second and third hours revealed by immunoblotting. Its retrieval is probably close to completion in ~10% of the (vacuolin-positive) phagosomes but barely started in the other 90%. As a consequence of this heterogeneity, the proportion of phagosomes lacking CatD never reaches zero, because at the time the early ones all acquire CatD, some are reaching the final phase when they become CatD-negative again. Nevertheless, because we classified ~2500 phagosomes, the concurrent decrease of phagosomes with intermediate and high levels of CatD and the rise of CatD-negative phagosomes seen at 3h is highly significant and cannot be easily generated by any mechanism other than recycling of CatD. It is not yet clear whether the rings of dots of CatD associated with the vacuolin-positive phagosomes represent clumps of CatD inside the phagosome, somehow concentrated in view of retrieval, or CatD-positive recycling vesicles lining up at the periphery of phagosomes.

Preliminary analysis of lipid composition revealed that phagosomes have a very distinct profile compared with bulk membranes. We consider these data as a proof of principle that a comprehensive lipidomics of phagosomes is at hand. For the first time, it might be possible to follow with great precision the time-dependent evolution of an endocytic organelle undergoing complex maturation, including multiple-signaling and membrane-trafficking events. This information will complement and synergize the protein-biased view of this process but will also allow a better understanding of the correlation between the various functions of that organelle and the biophysical constraints imposed on it through the sorting, fusion, fission, and transport events it undergoes. Together with lipidomics, our proteomic approach will strengthen the position of *D. discoideum* as a powerful model organism to study phagocytosis and will undoubtedly identify novel molecular players. In contrast to the mammalian systems, this first explorative phase will then be followed by a very efficient molecular genetics phase involving manipulation of the genes of interest, including by gene ablation and conditional expression of dominant mutants. This global strategy is likely to bring strong confirmation that *D. discoideum* is generally relevant for the unraveling of mechanisms of phagocytosis, because it involves many of the same components as in higher organisms, but it will surely turn up additional conserved factors such as coronin and myosin VII, the role of which in phagocytosis was first revealed in *D. discoideum* (de Hostos, 1999; Titus, 1999).

In conclusion, this initial molecular characterization of phagocytic mechanisms outlines the complexity of the numerous, distinct membrane trafficking events accompanying maturation and also establishes the reference for future comparison with genetically engineered phagocytic mutants.

ACKNOWLEDGMENTS

We thank all the present and past members of the Soldati laboratory, including Eva Neuhaus, who initiated the project. Britta Brügger and Felix Wieland provided invaluable preliminary analysis of the phagosome lipidome, and Thomas Ruppert and Armin Bosserhof were instrumental in the proteomic investigations. We thank Pierre Cosson, François Letourneur, and Meg Titus for constructive criticism of the manuscript. This work was supported by the Max-Planck Society, and Daniel Gotthardt was a self-supported medical student.

REFERENCES

Allen, L.H., and Aderem, A. (1995). A role for MARCKS, the alpha isozyme of protein kinase C and myosin I in zymosan phagocytosis by macrophages. J. Exp. Med. *182*, 829–840.

Allison, A.C., Davies, P., and De Petris, S. (1971). Role of contractile microfilaments in macrophage movement and endocytosis. Nat New Biol *232*, 153–155.

Bajno, L., Peng, X.-R., Schreiber, A.D., Moore, H.-P., Trimble, W.S., and Grinstein, S. (2000). Focal exocytosis of VAMP3-containing vesicles at sites of phagosome formation. J. Cell Biol. *149*, 697–705.

Beningo, K.A., and Wang, Y.L. (2002). Fc-receptor-mediated phagocytosis is regulated by mechanical properties of the target. J. Cell Sci. *115*, 849–856.

Bligh, E.G., and Dyer, W.J. (1959). A rapid method of total lipid extraction and purification. Can. J. Biochem. Physiol. *37*, 911–917.

Blocker, A., Severin, F.F., Burkhardt, J.K., Bingham, J.B., Yu, H., Olivo, J.C., Schroer, T.A., Hyman, A.A., and Griffiths, G. (1997). Molecular requirements for bi-directional movement of phagosomes along microtubules. J. Cell Biol. *137*, 113–129.

Bogdanovic, A., Bruckert, F., Morio, T., and Satre, M. (2000). A syntaxin 7 homologue is present in *Dictyostelium discoideum* endosomes and controls their homotypic fusion. J. Biol. Chem. 275, 36691–36697.

Bogdanovic, A., Bennett, N., Kieffer, S., Louwagie, M., Morio, T., Garin J., Satre, M., and Bruckert, F. (2002). Syntaxin 7, Syntaxin 8, Vti 1 and VAMP7 form an active SNARE complex for early macropinocytic compartment fusion in *Dictyostelium discoideum*. Biochem. J. *in press*.

Booth, J.W., Trimble, W.S., and Grinstein, S. (2001). Membrane dynamics in phagocytosis. Semin. Immunol. *13*, 357–364.

Brügger, B., Erben, G., Sandhoff, R., Wieland, F.T., and Lehmann, W.D. (1997). Quantitative analysis of biological membrane lipids at the low picomole level by nano-electrospray ionization tandem mass spectrometry. Proc. Natl. Acad. Sci. USA *94*, 2339–2344.

Buczynski, G., Bush, J., Zhang, L.Y., Rodriguez-Paris, J., and Cardelli, J. (1997). Evidence for a recycling role for Rab7 in regulating a late step in endocytosis and in retention of lysosomal enzymes in *Dictyostelium discoideum*. Mol. Biol. Cell 8, 1343–1360.

Cardelli, J. (2001). Phagocytosis and macropinocytosis in *Dictyostelium*: phosphoinositide- based processes, biochemically distinct. Traffic *2*, 311–320.

Caron, E., and Hall, A. (1998). Identification of 2 distinct mechanisms of phagocytosis controlled by different rho-GTPases. Science *282*, 1717–1721.

Castellano, F., Chavrier, P., and Caron, E. (2001). Actin dynamics during phagocytosis. Semin. Immunol. *13*, 347–355.

Chia, C.P. (1996). A 130-kDa plasma membrane glycoprotein involved in *Dictyostelium* phagocytosis. Exp. Cell Res. *227*, 182–189.

Chimini, G., and Chavrier, P. (2000). Function of Rho family proteins in actin dynamics during phagocytosis and engulfment. Nat. Cell Biol. *2*, E191–E196.

Claus, V., Jahraus, A., Tjelle, T., Berg, T., Kirschke, H., Faulstich, H., and Griffiths, G. (1998). Lysosomal enzyme trafficking between phagosomes, endosomes, and lysosomes in J774 macrophages: enrichment of cathepsin H in early endosomes. J. Biol. Chem. *273*, 9842–9851.

Cox, D., Lee, D.J., Dale, B.M., Calafat, J., and Greenberg, S. (2000). A Rab11-containing rapidly recycling compartment in macrophages that promotes phagocytosis. Proc. Natl. Acad. Sci. USA *97*, 680–685.

de Hostos, E.L. (1999). The coronin family of actin-associated proteins. Trends Cell Biol. *9*, 345–350.

de Hostos, E.L., Bradtke, B., Lottspeich, F., Guggenheim, R., and Gerisch, G. (1991). Coronin, an actin binding protein of *Dictyostelium discoideum* localized to cell surface projections, has sequence similarities to G protein beta subunits. EMBO J. *10*, 4097–4104.

Defacque, H., Egeberg, M., Antzberger, A., Ansorge, W., Way, M., and Griffiths, G. (2000). Actin assembly induced by polylysine beads or purified phagosomes: quantitation by a new flow cytometry assay. Cytometry *41*, 46–54.

Desjardins, M. (1995). Biogenesis of phagolysosomes: the "kiss and run" hypothesis. Trends Cell Biol. 5, 183–186.

Desjardins, M., Celis, J.E., van Meer, G., Dieplinger, H., Jahraus, A., Griffiths, G., and Huber, L.A. (1994a). Molecular characterization of phagosomes. J. Biol. Chem. *269*, 32194–32200.

Desjardins, M., Huber, L.A., Parton, R.G., and Griffiths, G. (1994b). Biogenesis of phagolysosomes proceeds through a sequential series of interactions with the endocytic apparatus. J. Cell Biol. *124*, 677–688.

Di, A., Krupa, B., Bindokas, V.P., Chen, Y., Brown, M.E., Palfrey, H.C., Naren, A.P., Kirk, K.L., and Nelson, D.J. (2002). Quantal release of free radicals during exocytosis of phagosomes. Nat. Cell Biol. *4*, 279–285.

Garin, J., Diez, R., Kieffer, S., Dermine, J.F., Duclos, S., Gagnon, E., Sadoul, R., Rondeau, C., and Desjardins, M. (2001). The phagosome proteome: insight into phagosome functions. J. Cell Biol. *152*, 165–180.

Gorg, A., Obermaier, C., Boguth, G., Harder, A., Scheibe, B., Wildgruber, R., and Weiss, W. (2000). The current state of two-dimensional electrophoresis with immobilized pH gradients. Electrophoresis *21*, 1037–1053.

Hackam, D.J., Botelho, R.J., Sjolin, C., Rotstein, O.D., Robinson, J.M., Schreiber, A.D., and Grinstein, S. (2001). Indirect role for COPI in the completion of FCgamma receptor-mediated phagocytosis. J. Biol. Chem. *276*, 18200–18208.

Jahraus, A., Egeberg, M., Hinner, B., Habermann, A., Sackman, E., Pralle, A., Faulstich, H., Rybin, V., Defacque, H., and Griffiths, G. (2001). ATP-dependent membrane assembly of F-actin facilitates membrane fusion. Mol. Biol. Cell *12*, 155–170.

Jahraus, A., Storrie, B., Griffiths, G., and Desjardins, M. (1994). Evidence for retrograde traffic between terminal lysosomes and the prelysosomal/late endosome compartment. J. Cell Sci. *107*, 145–157.

Janssen, K.P., Rost, R., Eichinger, L., and Schleicher, M. (2001). Characterization of CD36/LIMPII homologues in *Dictyostelium discoideum*. J. Biol. Chem. 276, 38899–38910.

Jenne, N., Rauchenberger, R., Hacker, U., Kast, T., and Maniak, M. (1998). Targeted gene disruption reveals a role for vacuolin-B in the late endocytic pathway and exocytosis. J. Cell Sci. *111*, 61–70.

Journet, A., Chapel, A., Jehan, S., Adessi, C., Freeze, H., Klein, G., and Garin, J. (1999). Characterization of *Dictyostelium discoideum* cathepsin D: molecular cloning, gene disruption, endo-lysosomal localization and sugar modifications. J. Cell Sci. *112*, 3833–3843.

Karakesisoglou, I., Janssen, K.P., Eichinger, L., Noegel, A.A., and Schleicher, M. (1999). Identification of a suppressor of the *Dictyostelium* profilin-minus phenotype as a CD36/LIMP-II homologue. J. Cell Biol. *145*, 167–181.

Laemmli, U.K. (1970). Cleavage of structural proteins during the assembly of the head of bacteriophage T4. Nature *227*, 680–685.

Laurent, O., Bruckert, F., Adessi, C., and Satre, M. (1998). In vitro reconstituted *Dictyostelium discoideum* early endosome fusion is regulated by Rab7 but proceeds in the absence of ATP-Mg^{2+} from the bulk solution. J. Biol. Chem. 273, 793–799.

Maniak, M. (1999). Endocytic transit in *Dictyostelium*. Protoplasma *210*, 25–30.

Maniak, M. (2001). Fluid-phase uptake and transit in axenic *Dictyostelium* cells. Biochim. Biophys. Acta *1525*, 197–204.

Metchnikoff, E. (1905). Immunity in Infective Diseases, Cambridge, London, Glasgow: Cambridge University Press.

Monnat, J., Hacker, U., Geissler, H., Rauchenberger, R., Neuhaus, E.M., Maniak, M., and Soldati, T. (1997). *Dictyostelium discoideum* protein disulfide isomerase, an endoplasmic reticulum resident enzyme lacking a KDEL-type retrieval signal. FEBS Lett. *418*, 357–362.

Muller, W.A., Steinman, R.M., and Cohn, Z.A. (1983). Membrane proteins of the vacuolar system. III. Further studies on the composition and recycling of endocytic vacuole membrane in cultured macrophages. J. Cell Biol. *96*, 29–36.

Neuhaus, E.M., Almers, W., and Soldati, T. (2002). Morphology and dynamics of the endocytic pathway in *Dictyostelium discoideum*. Mol. Biol. Cell 13, 1390–1407.

Neuhaus, E.M., Horstmann, H., Almers, W., Maniak, M., and Soldati, T. (1998). Ethane-freezing/methanol-fixation of cell monolayers: a procedure for improved preservation of structure and antigenicity for light and electron microscopies. J. Struct. Biol. *121*, 326–342.

Neuhaus, E.M., and Soldati, T. (1999). Molecular mechanisms of membrane trafficking: what do we learn from *D. discoideum* ? Protist *150*, 235–243.

Neuhaus, E.M., and Soldati, T. (2000). A myosin I is involved in membrane recycling from early endosomes. J. Cell Biol. *150*, 1013–1026.

Oh, Y.K., Alpuche-Aranda, C., Berthiaume, E., Jinks, T., Miller, S.I., and Swanson, J.A. (1996). Rapid and complete fusion of macrophage lysosomes with phagosomes containing *Salmonella typhimurium*. Infect. Immun. *64*, 3877–3883.

Pitt, A., Mayorga, L.S., Stahl, P.D., and Schwartz, A.L. (1992). Alterations in the protein composition of maturing phagosomes. J. Clin. Invest. *90*, 1978–1983.

Rabilloud, T., Adessi, C., Giraudel, A., and Lunardi, J. (1997). Improvement of the solubilization of proteins in two-dimensional

electrophoresis with immobilized pH gradients. Electrophoresis *18*, 307–316.

Rabilloud, T., Carpentier, G., and Tarroux, P. (1988). Improvement and simplification of low-background silver staining of proteins by using sodium dithionite. Electrophoresis *9*, 288–291.

Ramachandra, L., Song, R., and Harding, C.V. (1999). Phagosomes are fully competent antigen-processing organelles that mediate the formation of peptide:class II MHC complexes. J. Immunol. *162*, 3263–3272.

Rauchenberger, R., Hacker, U., Murphy, J., Niewohner, J., and Maniak, M. (1997). Coronin and vacuolin identify consecutive stages of a late, actin-coated endocytic compartment in *Dictyostelium*. Curr. Biol. *7*, 215–218.

Regula, J.T., Ueberle, B., Boguth, G., Gorg, A., Schnolzer, M., Herrmann, R., and Frank, R. (2000). Towards a two-dimensional proteome map of *Mycoplasma pneumoniae*. Electrophoresis *21*, 3765–3780.

Rosenfeld, J., Capdevielle, J., Guillemot, J.C., and Ferrara, P. (1992). In-gel digestion of proteins for internal sequence analysis after one- or two-dimensional gel electrophoresis. Anal. Biochem. *203*, 173–179.

Rouser, G., Fkeischer, S., and Yamamoto, A. (1970). Two dimensional then layer chromatographic separation of polar lipids and determination of phospholipids by phosphorus analysis of spots. Lipids *5*, 494–496.

Rupper, A., and Cardelli, J. (2001). Regulation of phagocytosis and endo-phagosomal trafficking pathways in *Dictyostelium discoideum*. Biochim. Biophys. Acta *1525*, 205–216.

Schwarz, E.C., Neuhaus, E.M., Kistler, C., Henkel, A.W., and Soldati, T. (2000). *Dictyostelium* myosin IK is involved in the maintenance of cortical tension and affects motility and phagocytosis. J. Cell Sci. *113*, 621–633.

Shevchenko, A., Wilm, M., Vorm, O., Jensen, O.N., Podtelejnikov, A.V., Neubauer, G., Mortensen, P., and Mann, M. (1996). A strategy for identifying gel-separated proteins in sequence databases by MS alone. Biochem. Soc. Trans. *24*, 893–896.

Souza, G.M., Mehta, D.P., Lammertz, M., Rodriguez-Paris, J., Wu, R.R., Cardelli, J.A., and Freeze, H.H. (1997). *Dictyostelium* lysosomal proteins with different sugar modifications sort to functionally distinct compartments. J. Cell Sci. *110*, 2239–2248.

Sussman, M. (1987). Cultivation and synchronous morphogenesis of *Dictyostelium* under controlled experimental conditions. Methods Cell Biol. *28*, 9–29.

Swanson, J.A., Johnson, M.T., Beningo, K., Post, P., Mooseker, M., and Araki, N. (1999). A contractile activity that closes phagosomes in macrophages. J. Cell Sci. *112*, 307–316.

Thilo, L. (1985). Quantification of endocytosis-derived membrane traffic. Biochim. Biophys. Acta *822*, 243–266.

Titus, M.A. (1999). A class VII unconventional myosin is required for phagocytosis. Curr. Biol. *9*, 1297–1303.

Troll, H., Malchow, D., Mueller-Taubenberger, A., Humbel, B., Lottspeich, F., Ecke, M., Gerisch, G., Schmid, A., and Benz, R. (1992). Purification, functional characterization, and cDNA sequencing of mitochondrial porin from *Dictyostelium discoideum*. J. Biol. Chem. *267*, 21072–21079.